

stress.

In spite of the various interesting open questions, we trust that this Letter has clarified the basic aspects of a very intriguing problem, and will contribute to a better understanding of Si surfaces.

We thank Hartwig Thomas for image processing, F. Himpsel for hints concerning sample preparation, and K. C. Pandey and K. H. Rieder for illuminating discussions on surface problems.

<sup>1</sup>Reviews of activities prior to 1980 are found in D. E. Eastman, *J. Vac. Sci. Technol.* **17**, 492 (1980); D. J. Chadi, *J. Phys. Soc. Jpn.* **49**, Suppl. A, 1035 (1980); D. J. Miller and D. Haneman, *Surf. Sci.* **104**, L237 (1980).

<sup>2</sup>J. C. Phillips, *Phys. Rev. Lett.* **45**, 905 (1980); R. J. Culbertson, L. C. Feldman, and P. J. Silverman, *Phys. Rev. Lett.* **45**, 2043 (1980); G. Le Lay, *Surf. Sci.* **108**,

L429 (1981); C. Y. Su, P. R. Skeath, I. Lindau, and W. E. Spicer, *Surf. Sci.* **107**, L355 (1981); M. J. Cardillo, *Chem. Phys.* **21**, 54 (1982); N. Garcia, *Solid State Commun.* **40**, 719 (1981); F. J. Himpsel, D. E. Eastman, P. Heimann, B. Reihl, C. W. White, and D. M. Zehner, *Phys. Rev. B* **24**, 1120 (1980); J. Pollmann, *Phys. Rev. Lett.* **49**, 1649 (1982); a trimer model has been proposed by F. J. Himpsel, to be published.

<sup>3</sup>G. Binnig, H. Rohrer, Ch. Gerber, and E. Weibel, *Appl. Phys. Lett.* **40**, 178 (1982), and *Phys. Rev. Lett.* **49**, 57 (1982); G. Binnig and H. Rohrer, to be published.

<sup>4</sup>F. J. Himpsel, private communication; see also P. A. Bennet and M. W. Webb, *Surf. Sci.* **104**, 74 (1981).

<sup>5</sup>L. C. Snyder, Z. Wassermann, and J. W. Moskowitz, *J. Vac. Sci. Technol.* **16**, 1266 (1979).

<sup>6</sup>W. A. Harrison, *Surf. Sci.* **55**, 1 (1976).

<sup>7</sup>K. C. Pandey, *Phys. Rev. Lett.* **49**, 223 (1982).

<sup>8</sup>J. Lander, in *Progress in Solid State Chemistry*, edited by H. Reiss (Pergamon, Oxford, 1965), Vol. 2, p. 26. This work is disputed; see F. Jona, *IBM J. Res. Dev.* **9**, 357 (1965). On the other hand, Sn on Ge leads to both a  $5 \times 5$  and a  $7 \times 7$  structure: T. Ichikawa and S. Ino, *Solid State Commun.* **27**, 483 (1978).

## Electronic and Magnetic Properties of Europium-Intercalated Graphite

G. Kaindl, J. Feldhaus, U. Ladewig, and K. H. Frank

*Institut für Atom- und Festkörperphysik, Freie Universität Berlin, D-1000 Berlin 33, Germany*

(Received 28 September 1982)

Stage-1 Eu-intercalated graphite  $\text{EuC}_6$  was studied by Mössbauer and  $L$ -edge spectroscopy. Isomer shift and  $L_{\text{III}}$ -edge position results indicate the divalent state for Eu. Below 40 K,  $\text{EuC}_6$  orders antiferromagnetically with the Eu spins oriented perpendicular to  $\vec{c}$  and a magnetic hyperfine field saturating at  $-10.7$  T. The large electric field gradient at the Eu site ( $-1.4 \times 10^{18}$  V/cm<sup>2</sup>), with axis parallel to  $\vec{c}$ , is consistent with the structure of  $\text{EuC}_6$  and a partial charge transfer from Eu to the C planes.

PACS numbers: 75.30.Kz, 76.80.+y, 78.70.Dm

The highly anisotropic magnetic properties of graphite intercalation compounds (GIC) are of considerable current interest.<sup>1,2</sup> By increasing the number of graphite layers separating the two-dimensional arrays of magnetic intercalants studies of the transition from three-dimensional to more and more two-dimensional magnetic behavior are feasible.<sup>3</sup> Most of the relevant work so far has dealt with transition-metal chlorides as magnetic intercalants, and substantial changes in the magnetic properties relative to those of the pure intercalants were observed.<sup>1-3</sup> With the demonstration of the feasibility of vapor-phase intercalation of Eu,<sup>4</sup> a magnetic intercalation system with bare magnetic ions became available, since Eu is expected to intercalate in its  $4f^7$ -

divalent magnetic state.<sup>5</sup> Higher-stage Eu GIC's should constitute prototypes for two-dimensional arrays of magnetic ions with almost isotropic exchange. Up to now only the results of magnetization measurements<sup>5</sup> and Raman studies<sup>6</sup> have been published for  $\text{EuC}_6$ .

The present paper reports on a <sup>151</sup>Eu Mössbauer study of  $\text{EuC}_6$  as well as on  $L$ -edge x-ray absorption and magnetic measurements. From the observed Mössbauer isomer shift and the position of the  $L_{\text{III}}$  edge Eu is shown to be intercalated in its divalent state. The magnitude, negative sign, and orientation of the axially symmetric electric-field gradient (EFG) tensor at the Eu site are in quantitative agreement with the crystallographic structure of  $\text{EuC}_6$ .<sup>4</sup> Below 40 K the Mössbauer

spectra exhibit a combined magnetic–electric–quadrupole hyperfine interaction due to long-range magnetic order, with the Eu spins oriented in the basal plane of graphite. Magnetization measurements, which are in accord with recently published work,<sup>5</sup> reveal antiferromagnetic order.

The Mössbauer experiments were performed in transmission geometry with a  $^{151}\text{SmF}_3$  source. For the  $L_{\text{III}}$ -edge measurements an x-ray absorption spectrometer based on a focusing monochromator and a 2-kW x-ray source was employed.<sup>7</sup> Magnetic data were taken with a vibrating-sample magnetometer. The  $\text{EuC}_6$  samples were prepared by vapor-phase intercalation in sealed Mo or quartz containers from natural graphite flakes or highly oriented pyrolytic graphite (HOPG) and 99.99%-pure Eu metal. The samples were intercalated up to 20 d at 520 °C. X-ray analysis revealed the dominant presence of stage-1  $\text{EuC}_6$  with a  $c$ -axis periodicity of 4.87 Å, in addition to pristine graphite. The Eu GIC's were handled in purified inert-gas atmosphere.

Figure 1 shows a Mössbauer spectrum and an  $L_{\text{III}}$ -edge spectrum, taken from Eu-intercalated natural graphite flakes at 300 K (sample  $\text{EuC}_6$  No.

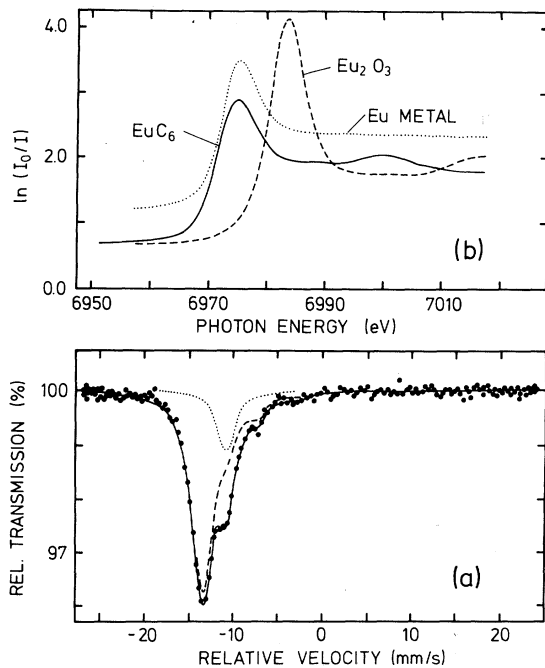


FIG. 1. (a)  $^{151}\text{Eu}$  Mössbauer spectrum and (b)  $L_{\text{III}}$ -edge spectrum (solid curve) of  $\text{EuC}_6$  (sample No. 2) at 300 K. The solid line in (a) represents the result of a least-squares fit (see text). In (b) the  $L_{\text{III}}$  edges of typical  $\text{Eu}^{2+}$  and  $\text{Eu}^{3+}$  solids are also shown.

2). The Mössbauer spectrum, which is characterized by a pure  $\text{Eu}^{2+}$  signal of the  $21.6\text{-keV } \frac{5}{2} \rightarrow \frac{7}{2} \gamma$  transition, was least-squares fitted (solid line) by a superposition of an electric-quadrupole-split subspectrum (dashed curve, composed of eight individual lines) and a single absorption line (dotted curve). The main subspectrum originates from  $\text{EuC}_6$  and is described by an isomer shift  $S = -11.7 \pm 0.1$  mm/s and an axially symmetric EFG tensor  $V_{zz} = -(1.4 \pm 0.1) \times 10^{18}$  V/cm<sup>2</sup> [corresponding to  $eV_{zz}Q(\frac{5}{2}) = -389$  MHz]. The weaker, dotted subspectrum ( $\cong 25\%$  intensity) is described by a single Lorentzian at  $S = -11.3 \pm 0.2$  mm/s and is due to  $\text{EuO}$  and  $\text{Eu-carbide (EuC}_x)$  impurity phases (see below). From the relative intensities of the eight components of the electric-quadrupole-split  $\text{EuC}_6$  subspectrum there follows a strong texture of the absorber with the graphite  $c$  axis oriented predominantly perpendicular to the absorber plane. Therefore, a Mössbauer spectrum taken with the same absorber tilted by  $45^\circ$  relative to the  $\gamma$ -ray direction (not shown here) revealed that the axis of the EFG tensor is directed parallel to  $\bar{c}$ . This is expected from the structure of  $\text{EuC}_6$ , since for an  $s$ -state ion like  $\text{Eu}^{2+}$  the EFG is caused only by the lattice, providing a direct measure of the crystalline anisotropy.

In Fig. 1(b) the  $L_{\text{III}}$ -edge spectra of divalent Eu metal (dotted curve) and of trivalent  $\text{Eu}_2\text{O}_3$  (dashed curve) are shown in addition to the one of  $\text{EuC}_6$ . The  $L_{\text{III}}$  edges are characterized by an intense peak at the absorption threshold ("white line") due to transitions from a  $2p$  initial state to empty  $5d$  states at  $E_F$ . The  $L_{\text{III}}$ -edge position is mainly determined by the  $4f$  occupation number, reflecting the difference of  $\cong 8$  eV in  $2p$  binding energies between the  $4f^7$  and  $4f^6$  configurations of Eu.<sup>8</sup> Chemical effects are expected to vary the  $L_{\text{III}}$ -edge position by less than 1 eV. Therefore, the  $L_{\text{III}}$ -edge position confirms the divalent character of  $\text{EuC}_6$ .

Low-temperature Mössbauer spectra taken from the same sample are shown in Fig. 2. The 77-K resonance curve is essentially identical to the 300-K spectrum of Fig. 1(a), while those taken at 30 K and below are dominated (dashed  $\text{EuC}_6$  subspectrum) by a combined electric–quadrupole–magnetic–dipole hyperfine interaction with a small hyperfine field  $B_{\text{eff}} (-10.7$  T at 4.2 K). The weak, dotted subspectrum from  $\text{EuC}_x$  and  $\text{EuO}$  impurity phases can be described by a pure magnetic hyperfine interaction with a large field  $B_{\text{eff}} = -(29.5 \pm 1)$  T and  $S = -11.3$  mm/s. In the least-squares-fit analysis the angle  $\theta$

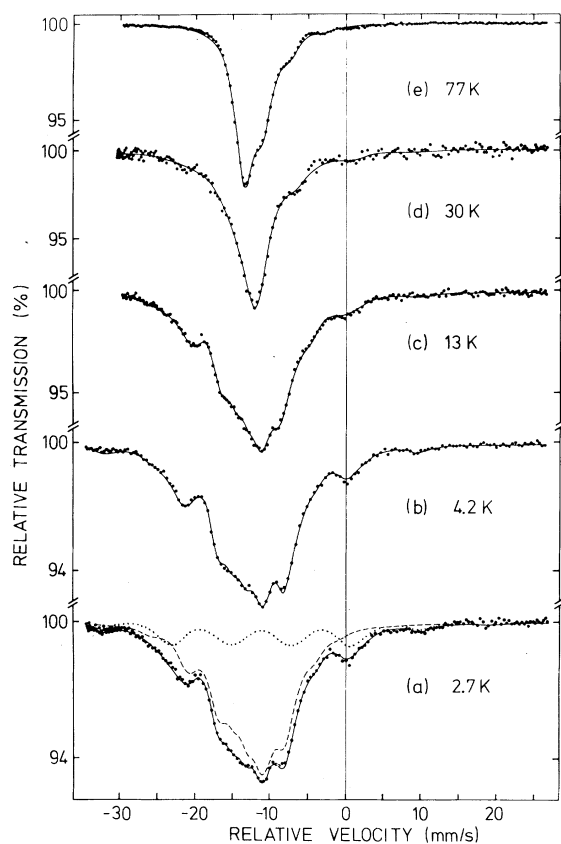


FIG. 2. Mössbauer spectra of  $\text{EuC}_6$  (sample No. 2) at various temperatures. The solid lines are fit results. The dashed subspectrum in (a) stems from  $\text{EuC}_6$ , and the dotted one from  $\text{EuC}_x$  and  $\text{EuO}$  impurity phases.

between the axis of the EFG tensor and  $B_{\text{eff}}$  in  $\text{EuC}_6$  was treated as a free parameter, resulting in  $\theta = (90 \pm 5)^\circ$ . This means that the *Eu spins are oriented in the basal plane of graphite in the magnetically ordered phase of  $\text{EuC}_6$* . A paramagnetic state with slow spin-lattice relaxation can be ruled out for the following reasons: (i) the small magnitude and the low-temperature saturation behavior of  $B_{\text{eff}}$  and (ii) the nonisotropic orientation of  $B_{\text{eff}}$  with respect to the EFG axis.

We have taken 300-K spectra of five and low-temperature spectra of two separately prepared  $\text{EuC}_6$  samples (No. 2 and No. 9) with consistent results. Only the relative intensity of the impurity-phase subspectrum varied slightly among samples. In order to identify better the chemical nature of the weak impurity phase we have studied  $\text{Eu}$  carbide samples prepared from the elements in closed Mo crucibles at 900 and 1200  $^\circ\text{C}$ , respectively. The tetragonal  $\text{EuC}_2$ <sup>9</sup> obtained at 1200  $^\circ\text{C}$  orders ferromagnetically at  $\cong 22$  K, while the carbide prepared at 900  $^\circ\text{C}$  was found to

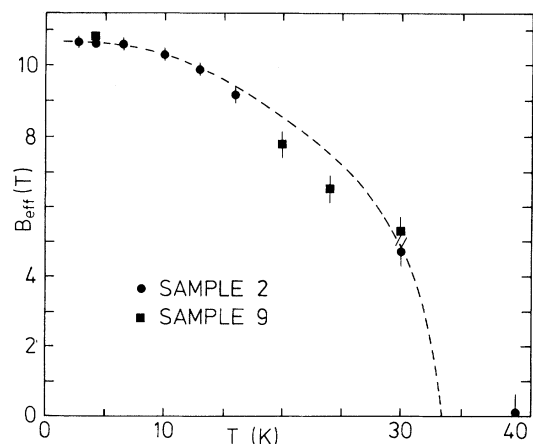


FIG. 3. Temperature dependence of the magnetic hyperfine field at  $^{151}\text{Eu}$  in  $\text{EuC}_6$ , together with a Brillouin ( $S = \frac{7}{2}$ ) fit (dashed curve).

order at  $\cong 13$  K. The 4.2-K Mössbauer spectra of both carbides are practically identical, with  $B_{\text{eff}} = -30.5 \pm 1$  T,  $S = -(11.3 \pm 0.2)$  mm/s, and a small positive EFG. These hyperfine parameters are very similar to those of  $\text{EuO}$ ,<sup>10</sup> and are compatible with the spectral parameters for the impurity phase in our  $\text{EuC}_6$  samples. In the magnetization measurements (not shown here) steps at 69 K (due to  $\text{EuO}$ ), 22 K, and 13 K (due to  $\text{EuC}_x$  impurities) were clearly observed in the samples prepared from natural graphite flakes (No. 2 and No. 9); no  $\text{EuO}$ , however, could be found in an  $\text{EuC}_6$  sample prepared from HOPG. The  $\text{EuC}_x$  and  $\text{EuO}$  impurities can be distinguished in the Mössbauer spectra by their rather different magnetization temperatures. This resulted for the  $\text{EuC}_6$  sample No. 2 in an  $\text{EuC}_x$  ( $\text{EuO}$ ) content of  $\cong 12\%$  ( $\cong 13\%$ ), in agreement with our magnetization measurements.

The results for the temperature dependence of  $B_{\text{eff}}$  obtained from two different samples are plotted in Fig. 3.  $B_{\text{eff}}$  is expected to be proportional to the local magnetization at the  $\text{Eu}$  site. The dashed line represents a fit with a three-dimensional molecular-field Brillouin ( $S = \frac{7}{2}$ ) curve, resulting in a magnetic ordering temperature of  $\cong 34$  K, which has to be considered as a lower limit. In Ref. 5 a value of  $T_N = 40$  K was given on the basis of magnetization measurements.

The magnetization measurements of Ref. 5 as well as our own show that  $\text{EuC}_6$  orders antiferromagnetically. In addition, we learned in the present work that the  $\text{Eu}$  spins are oriented within the intercalant planes. There is strong indication from the metamagnetic transitions observed

in external fields up to 35 T (Ref. 5) that the long-range antiferromagnetic order exists *within the Eu planes*. We can therefore describe  $\text{EuC}_6$  as a quasi-isotropic layered Heisenberg antiferromagnet,<sup>11</sup> where a small anisotropy in the magnetic exchange may be due to dipolar and crystalline-electric fields; in addition, a weak interlayer exchange has to be expected. As can be seen in Fig. 3,  $B_{\text{eff}}$  falls off more rapidly with temperature than described by the Brillouin curve. This is actually expected for such a layered magnetic system because of a higher density of low-energy magnons as compared with the isotropic three-dimensional case.<sup>11</sup>

The isomer shift of  $\text{EuC}_6$  is the most negative one observed for any metallic  $\text{Eu}^{2+}$  system.<sup>10</sup> It reflects the relatively small *s*-like conduction-electron density at Eu due to partial charge transfer to the C planes and strong hybridization of the intercalant-layer conduction bands.<sup>12</sup> A strong hybridization can also be inferred from the shape of the Eu  $L_1$  edge in  $\text{EuC}_6$ ,<sup>7</sup> which depends on the local  $p$  density of empty conduction-band states.

Both the electronic and the lattice structures of  $\text{EuC}_6$  are reflected in the EFG tensor. The magnitude of  $V_{zz}$ , which does not change with temperature, is the largest one observed for any  $\text{Eu}^{2+}$  compound,<sup>13</sup> reflecting the strong lattice anisotropy of  $\text{EuC}_6$ . It is mainly caused by the positively charged in-plane Eu neighbors and was reproduced quantitatively by a point-charge calculation based on the structure of  $\text{EuC}_6$  using a lattice Sternheimer factor of  $-72$ .<sup>14</sup>

Finally we discuss the saturation value of  $B_{\text{eff}}(T \rightarrow 0) = -10.7 \pm 0.2$  T. The sign was deduced from the observed decrease in the total magnetic splitting in strong external fields up to 6 T. In  $\text{Eu}^{2+}$  compounds the size of the Eu moment cannot be inferred from  $B_{\text{eff}}$  because of large contributions from conduction-electron polarization by the  $4f$  moment itself ( $B_s$ ) and from transferred hyperfine fields ( $B_t$ ), in addition to a rather chemically indifferent core-polarization field,  $B_c = -(34 \pm 2)$  T.<sup>15</sup> In order to explain the

relatively small magnitude of  $B_{\text{eff}}$  for  $\text{EuC}_6$ , we have to assume large positive contributions from  $B_s$  and  $B_t$ . In other magnetically ordered metallic Eu systems  $B_s$  was found to vary between  $+5$  and  $+19$  T, and large positive  $B_t$  contributions were found for compounds like  $\text{EuPt}_2$  and  $\text{EuPd}_2$ .<sup>15</sup> A quantitative analysis of  $B_{\text{eff}}$  must wait for detailed results on the spin structure of  $\text{EuC}_6$ .

The authors wish to thank Dr. B. Perscheid, Professor I. Nowik, P. Schmidt, and G. Wisny for various contributions, as well as Dr. A. W. Moore of Union Carbide for the HOPG material. The work was supported by the Sonderforschungsbereich-161 of the Deutsche Forschungsgemeinschaft.

<sup>1</sup>Yu S. Karimov, Zh. Eksp. Teor. Fiz. **68**, 1539 (1976) [Sov. Phys. JETP **41**, 772 (1976)].

<sup>2</sup>M. Elaky, C. Nicolini, G. Dresselhaus, and G. O. Zimmermann, Solid State Commun. **41**, 289 (1982).

<sup>3</sup>M. R. Corsow, S. E. Millmann, and G. R. Hoy, Solid State Commun. **42**, 667 (1982).

<sup>4</sup>M. El Makrini, D. Guérard, P. Lagrange, and A. Hérold, Physica (Utrecht) **99B**, 481 (1980).

<sup>5</sup>H. Suematsu *et al.*, Solid State Commun. **40**, 241 (1981), and **38**, 1103 (1981).

<sup>6</sup>D. M. Hwang and D. Guérard, Solid State Commun. **40**, 759 (1981).

<sup>7</sup>J. Feldhaus, Ph.D. thesis, Freie Universität Berlin, 1982 (unpublished).

<sup>8</sup>J. F. Herbst and J. W. Wilkins, Phys. Rev. B **26**, 1689 (1982).

<sup>9</sup>R. E. Gebelt and H. A. Eick, Inorg. Chem. **3**, 335 (1964).

<sup>10</sup>E. R. Bauminger, G. M. Kalvius, and I. Nowik, in *Mössbauer Isomer Shifts*, edited by G. K. Shenoy and F. E. Wagner (North-Holland, Amsterdam, 1978), p. 661.

<sup>11</sup>M. E. Lines, Phys. Chem. Solids **31**, 101 (1970).

<sup>12</sup>See, e.g., M. S. Dresselhaus and G. Dresselhaus, Adv. Phys. **30**, 139 (1981).

<sup>13</sup>See, e.g., C. L. Chien and A. W. Sleight, Phys. Rev. B **18**, 2031 (1978).

<sup>14</sup>R. P. Gupta and S. K. Sen, Phys. Rev. A **7**, 850 (1973).

<sup>15</sup>See, e.g., H. Kropp, W. Zipf, E. Dormann, and K. H. Buschow, J. Magn. Magn. Mater. **13**, 224 (1979).